oC8

STUDY OF THE VALIDITY OF A SHOCK WAVE MODEL TO DESCRIBE THE LASER-INDUCED PLASMA EXPANSION INTO OXYGEN GAS

S. LAFANE, T. KERDJA, S. ABDELLI-MESSACI and S. MALEK
Centre de Développement des Technologies Avancées,
Cité 20 août 1956, B.P. 17, Baba Hassen, Algérie
E-mail : slafane@cdta.dz

Abstract: In this contribution, the plume expansion dynamics of an ablated Sm_2O_3, Nd_2O_3 and NiO mixed oxide target by a KrF laser into a background of oxygen atmosphere has been investigated using fast ICCD imaging. The laser fluence was fixed at 2 Jcm^{-2} and the surrounding ambient gas pressure was varied from vacuum to 50 mbar. The imaging data were used to create position–time plots of the luminous front. The plume behaviour was found influenced by the gas pressure above a certain threshold. The plasma plume dynamics was analysed in the framework of a shock wave model. It was found that the shock wave model is valid at distance ranges which depend on the gas pressure. This was very well illustrated using dimensionless variables. By studying the evolution of the plume stopping distance at high pressures and comparing the measured plume mass to the calculated ones, it was found that the previsions of the shock wave model are valid.

Keywords: laser ablation, $Sm_{1-x}Nd_xNiO_3$, fast imaging, plume dynamics, shock wave

1. Introduction

Due to its metal–insulator transition and thermochromic properties, the rare earth-nickelate perovskite $RNiO_3$ (R ≠ La), has received a great deal of attention [1].The metal–insulator transition temperature (T_{MI}) can be tuned by changing the R cation. The interesting property is the ability to tune the T_{MI} in the wide range of temperature, especially around the ambient, by adjusting the relative ratio of the cations (R and R') in the $R_{1-x}R'_xNiO_3$ compound [2, 3].

Pulsed laser ablation is a technique for thin films deposition which is used to synthesise a variety of materials such as oxides [4, 5]. The main advantages of this technique are the stoichiometric transfer of the multicomponent target elements to substrate and the high kinetic energy of the ejected material to be deposited. Nevertheless, an optimisation of the deposition parameters, such as laser fluence, repetition rate and target to substrate distance, is needed to achieve a high films quality. In the case of oxides, as the oxygen is volatile, the deposition under oxygen atmosphere is required. Thus, the oxygen gas pressure is another parameter to optimise.

Several studies have been reported on the dynamics of the plasma plume in a background gas [6-12]. It was found that the plume dynamics is strongly affected by this latter. Several models have been proposed to describe this dynamics. Among these models, shock wave model [11, 13-17] is widely used in the literature.

In this work, we study the effect of oxygen pressure, for a given laser fluence, on the plasma plume dynamics for $Sm_{1-x}Nd_xNiO_3$ thin films deposition, using fast imaging. Also, we discuss the validity of the shock wave model to describe the dynamics of the plasma expansion into oxygen gas.

2. Experimental

The schematic of the experimental set-up is illustrated in Fig.1. The vacuum chamber was evacuated first by a turbomolecular pump to a residual pressure of 3×10^{-6} mbar and than filled with oxygen gas. Two cylindrical lenses are used to focus the KrF ($\lambda = 248$ nm, $\tau = 25$ ns) laser beam on the rotating target with an incident angle of 45°. The target is a mixture of samarium, neodymium and nickel oxide. The relative ratio of neodymium ($x = 0.45$) is set to have a T_{MI} close to room temperature (310 K). A set of spherical and plane mirrors and a Zeiss lens (76 mm focal length, spectral response: 350-800 nm) are used to form a two-dimensional image of the luminous plasma on the ICCD camera (Princeton Instruments PI-MAX, 1024 × 256 pixels, pixel size = 26 × 26 µm). The temporal resolution of the ICCD camera is 5 ns and its spectral response is within the range of 190–850 nm. The observation was made along the normal to the ejected material direction of propagation.

The study was carried out from vacuum to 50 mbar of oxygen gas pressures. The fluence was fixed at 2 J.cm^{-2}. The number of accumulation, ICCD gain and gate are adjusted for each image to compensate the reduction of the plume intensity during the expansion. The target surface and the end of the laser pulse were tacked as the origin of distances and time delays.

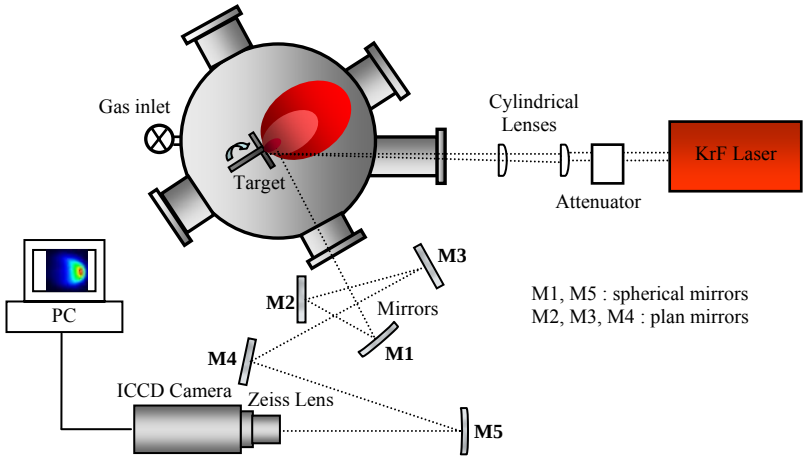

Figure 1 : Schematic of the experimental set-up

3. Results and discussion

Typical ICCD images of the temporal evolution of the expanding plasma plume into vacuum and four representative oxygen pressures are given in Figure 2. Each image represents the spectrally integrated emission in the range of 350-800 nm of the plasma plume excited species.

First, in a vacuum or low background pressure, the plume propagates freely. By increasing the oxygen pressure, the expansion dynamics of the plume is strongly affected by the interaction with the background gas. As shown in Figure 2, the plume propagation is progressively slowed down, compared to vacuum expansion, and the following effects are clearly distinguished: (i) spatial confinement of the species with the formation of a contact front, and a consequent increase of the emission at the front; (ii) double plume splitting and plume sharpening, in a defined time interval, depending on the pressure; (iii) plume stopping and transition to a diffusive-like propagation regime, at longer time delays and high pressure. Plume splitting marks the beginning of the interaction between the ejected species and the background gas molecules. The splitting appears only above a certain threshold pressure. In our case, this occurs at around 2×10^{-2} mbar. As the time evolves, the second component (the

slower one) joins the first component, because of the background gas braking of the latter, and the plume splitting disappears. The plume splitting has already been reported by several authors [6, 9, 18]. This splitting is explained in [18] as a result of the interaction between the plume species which are scattered in backward direction after collisions with background gas molecules and the incoming particles. As time evolves and for some range of pressures, at around 0.5 mbar, a sharpening of the plume appears. Plume sharpening behaviour suggests that higher kinetic energy particles are emitted closer to the target surface normal [9]. Along with the sharpening, the plume splits again into two components. This second splitting is clearly observed at 0.5-5 mbar pressure range. It was attributed to the deceleration of a part of the plasma plume due to the interaction with background gas [9] or due to the formation of molecular species as reported by Kushwaha *et al* [13].

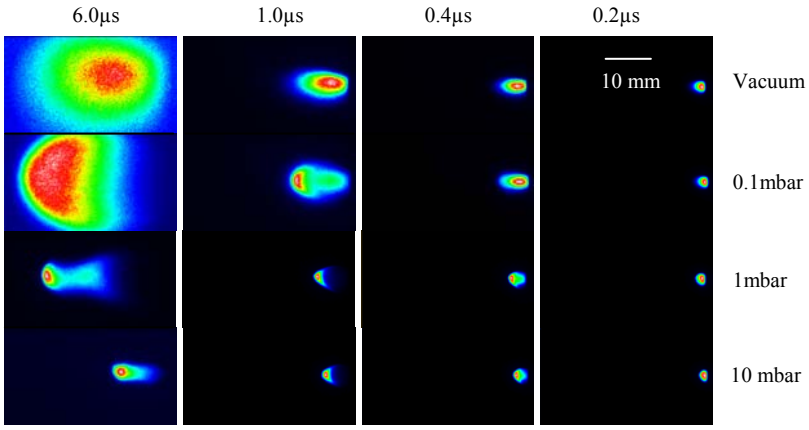

Figure 2 : Temporal evolution of the visible plume (the position of the ablating surface is at the limit of the top side of the images).

In order to study the plasma plume expansion dynamics, we plotted the plume luminous front position versus time delay at different O_2 pressures (see Figure 3). In vacuum and up to few hundredths of mbar the plasma plume expansion is linear. By increasing the pressure, the expansion remains linear in the early time. From vacuum to 1 mbar no change in the initial velocity was observed. We estimated this velocity to be around 1.7×10^6 cm/s. From 2 mbar to 35 mbar the initial velocity decreases from 1.25×10^6 to 0.75×10^6 cm/s. As the time evolves a deviation from free-plume expansion occurs and the plume slows down.

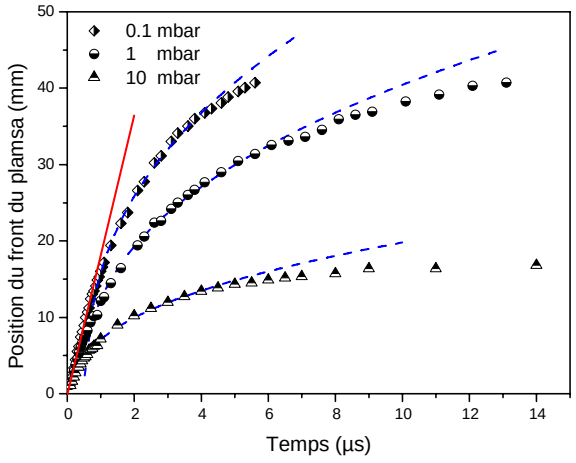

Figure 3 : Plume front position as a function of the time delay at 0.1, 1 and 10 mbar O_2 pressure. The solid line represents the free expansion and the dashed line the shock-wave model fit.

Several models have been proposed to describe the ablation plume expansion in a background gas. The deviation from the free-plume expansion and the appearance of luminous layer in the plasma-gas interface marks the presence of a shock front. The shock-wave model describes this regime of expansion. It assumes that the ejected material acts as a piston on gas, compresses it and puts it in motion forming a shock-wave. The position of shock front for spherical-wave propagation is given by [19]:

$$R(t) = \xi_0 \left(\frac{E}{\rho_0} \right)^{1/5} (t - t_0)^{2/5} \tag{1}$$

where ξ_0 is a parameter related to both geometric and thermodynamic quantities, E is the energy of the plume, ρ_0 is the undisturbed gas density, and t_0 is the boundary condition for the delayed shock-wave. We used equation (1) to fit our experimental data in order to verify the validity of the shock wave model. It was found that for all used pressures the fits agree well with a limited range of the experimental data. By increasing the pressure, the lower and the higher limit of distances where the shock-wave model is valid decreases as we can see on Figure 4 where the natural logarithm of distances as a function of the natural logarithm of time delays is represented. At 0.1, 1 and 10 mbar the lower limit is 15, 10 and 3.5 mm, respectively. According to [17] the validity of the shock wave model is restricted to a distance region where the mass of the gas surrounding the shock wave is higher than the mass of the ablated material up to distances at which the pressure driving the moving of the plasma plume is greater than the pressure of the gas at rest.

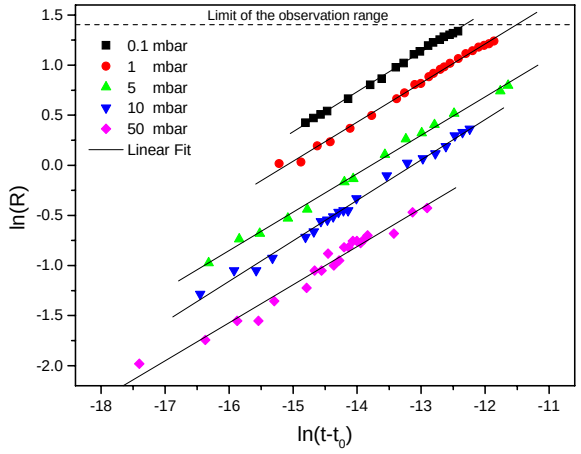

Figure 4 : Plume front position versus time delay at distances and time delays ranges where the shock-wave model is available.

In order to illustrate the different regime of the plume expansion into back-ground oxygen gas pressure, we used the dimensionless distance-time variables proposed by Arnolds *et al.* [20] to plot our experimental data, (see figure 5). These dimensionless variables are given as follow:

$$\bar{R} = R\left(\frac{2E}{P_0} \right)^{\frac{-1}{3}}, \bar{t} = tc_s \left(\frac{2E}{P_0} \right)^{\frac{-1}{3}} \tag{2}$$

where c_s is the sound velocity in the back-ground gas. As it is illustrated in Figure 5 all the curves for different pressures collapse onto an almost single one. The different stages of the plume expansion: the free expansion; the shock wave like expansion and finely the plume stopping, are clearly seen.

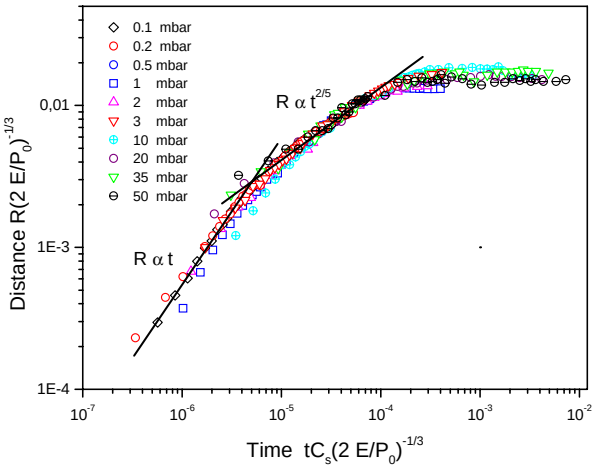

Figure 5 : Plume front position versus time delay at different background oxygen pressures in the dimensionless variables.

Figure 6 shows the evolution of the observed plume stopping distance versus oxygen gas pressure. According to Amoruso *et al.* [15, 18] the plume stops when the shock-wave gradually degenerates into a sound wave in the undisturbed gas, and almost all the energy initially stored in the plume (E_p) is converted into a sound wave propagating into the ambient gas. By considering a hemispherical plume expansion, the stopping condition reads: $E \approx 2/3\pi\rho_0 R_{st}^3 c_s^2$. This leads to the dependence of the stopping distance on the pressure $R_{st} \propto P^{-1/3}$, which is in very good agreement with our experimentally observed dependence in 2-5 mbar pressure range. For the higher pressures, we have found that the dependence is $R_{st} \propto P^{-0.58}$. We think that this is due to the energy spent in nanoparticules and shock-wave formation.

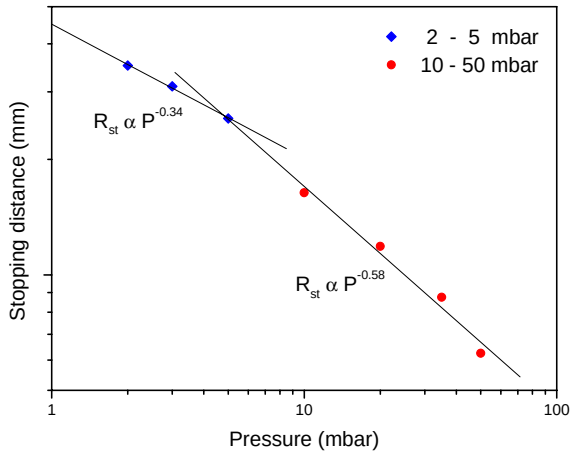

Figure 9. Plume stopping distance as a function of the background pressure.

According to Zel'dovich and Raiser [21], shock-wave formation becomes important when the mass of the displaced gas is comparable to the masse M_p of the plasma. Assuming a hemispherical expansion of the plume, it occurs for a front radius R_{sw} such as [15]:

$$(2/3)\pi R_{sw}^3 \rho_0 \approx M_p \tag{3}$$

Using equation (3) and tacking R_{sw} as the front position at which the beginning of the shock-wave formation was observed, M_p was calculated for all the used pressures and compared to the measured ablated mass in Figure 6. The plasma mass was measured by weighing the target before and after irradiation with 6000 laser pulse and was found equal to 1.13 µg. The M_p calculated values are closed to the measured value particularly at low pressures.

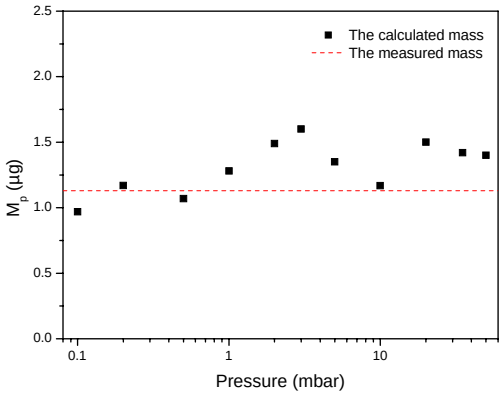

Figure 6 : Calculated plume mass compared to the measured mass (the dashed line) for the different pressures used.

4. Conclusion

The plume expansion dynamics of an ablated Sm_2O_3, Nd_2O_3 and NiO mixture oxides target by a KrF laser in a background oxygen atmosphere has been investigated using a fast ICCD imaging. Images analysis revealed several effects: double plume splitting, plume sharpening and plume stopping. The plume expansion passes from free-like to shock-like and finally reaches a complete stopping at times and distances depending on the gas pressure. The validity if the shock-wave model to describe plume dynamics into background oxygen pressure was studied. It was found that this model describe very well the plume dynamics in a limited distance region which depends on the gas pressure. This was very well illustrated using the dimensionless variables. By studying the evolution of the plume stopping distance at high pressures and comparing the measured plume mass to the calculated ones, it was found that the previsions of the shock-wave model are valid.

References

[1] M. L. Medarde : *J. Phys.: Condens. Matter* **9**, 1707 (1997)
[2] G. Frand, O. Bohnké, P. Lacorre, J. L. Fourquet, A. Carré, B. Eid, J. G. Theobald and A. Gire: J. Solid State Chem., **120**, 157 (1995)
[3] A. Ambrosini, J.F. Hamet: Appl. Phys. Lett. **82**, 727 (2003)
[4] D.B. Chrisey, G.K. Hubler (Eds.): Pulsed laser deposition of thin films (John Wiley and Sons, New York, 1994)
[5] D. Bauerle: Laser Processing and Chemistry (third ed., Springer, Berlin, 2000)

[6] D. B. Geohegan: Appl. Phys. Lett. **60**, 2732 (1992)
[7] D. B. Geohegan: Appl. Phys. Lett. **67**, 197 (1995)
[8] Hai-jun Dang, Qi-zong Qin : Appl. Surf. Sci. **151**, 180 (1999)
[9] S. S. Harilal, C. V. Bindhu, M. S. Tillak, F. Najmabadi, A. C. Gaeris: J. Appl. Phys. **93**, 2380 (2003)
[10] S. Amoruso, A. Sambri, W. Wang: J. Appl. Phys. **100**, 013302 (2006)
[11] S. Lafane, T. Kerdja, S. Abdelli-Messaci, S. Malek, M. Maaza, Appl. Phys. A, in press DOI 10.1007 (2009).
[12] S. Lafane, T. Kerdja, S. Abdelli-Messaci, S. Malek, M. Maaza, Appl. Surf. Sci. In Press (2009)
[13] A. Kushwaha, R. K. Thareja, Applied Optics, **47**, G65 (2008)
[14] T. E. Itina, J. Hermann, P. Delaporte, and M. Sentis: Phys. Rev. E, **66**, 066406 (2002)
[15] S. Amoruso, R. Bruzzesi, N. Spinelli, R. Velotta, M.Vitiello, and X. Wang: Phys. Rev. B **67**, 224503 (2003)
[16] C. Phelps, C. J. Druffner, G. P. Perram, R. R. Biggers, J. Phys. D: Appl. Phys. **40**, 4447 (2007).
[17] P.E. Dyer, J. Sidhu: J. Appl. Phys. **64**, 4657 (1988)
[18] S. Amoruso, A. Sambri, M. Vitiello, W. Wang: Appl. Surf. Sci. **252**, 4712 (2006)
[19] J. Gonzalo, C. N. Afonso, I. Madariaga: J. Appl. Phys. **88**, 951 (1997)
[20] N. Arnold, J. Gruber, J. Heitz: Appl. Phys. A **69**, S87 (1999)
[21] Ya. B. Zel'dovich and Yu. P. Raizer: Physics of Shock Waves and High-Temperature Hydrodynamic Phenomena (Academic, New York, 1966)